nature climate change

LETTERS

PUBLISHED ONLINE: 21 OCTOBER 2012 | DOI: 10.1038/NCLIMATE1722

Management of trade-offs in geoengineering through optimal choice of non-uniform radiative forcing

Douglas G. MacMartin[1]*, David W. Keith[2], Ben Kravitz[3] and Ken Caldeira[3]

Solar radiation management could be used to offset some or all anthropogenic radiative forcing, with the goal of reducing some of the associated climatic change[1,2]. However, the degree of compensation will vary, with residual climate changes larger in some regions than others. Similarly, the insolation reduction that best compensates climate changes in one region may not be the same as for another, leading to concerns about equity[3]. Here we show that optimizing the latitudinal and seasonal distribution of solar reduction can improve the fidelity with which solar radiation management offsets anthropogenic climate change. Using the HadCM3L general circulation model, we explore several trade-offs. First, residual temperature and precipitation changes in the worst-off region can be reduced by 30% relative to uniform solar reduction, with only a modest impact on global root-mean-square changes; this has implications for moderating regional inequalities. Second, the same root-mean-square residual climate changes can be obtained with up to 30% less insolation reduction, implying that it may be possible to reduce solar radiation management side-effects and risks (for example, ozone depletion if stratospheric sulphate aerosols are used). Finally, allowing spatial and temporal variability increases the range of trade-offs to be considered, raising the question of how to weight different objectives.

Multiple studies have explored the climate impacts of geoengineering[4–7], with several focusing in particular on regional disparities[3,8,9]. In a high-CO_2 world, using solar radiation management (SRM) can lead to a climate with temperature and precipitation that are closer in most regions to the baseline (current or pre-industrial) climate than not using SRM. However, the pattern of climate changes due to SRM does not fully match those due to increased CO_2, both because the different mechanisms of radiative forcing have different relative impacts on temperature versus precipitation[10], and the spatial and temporal distribution of radiative forcing obtained by uniform solar reduction does not match that due to increased CO_2 (ref. 4). As a result, the level of solar insolation reduction that best compensates climate change varies regionally[9]; similarly, for a given choice of insolation reduction, the degree of climate change compensation varies regionally. The analysis in ref. 9 is extended in ref. 3 to consider the optimal level of insolation reduction that minimizes either the area-weighted, population-weighted, or economy-weighted difference between the high-CO_2 world and the desired climate, exploring the question of whether different goals lead to different results.

However, both these and most other studies have introduced only a single degree-of-freedom perturbation in radiative forcing; this is typically uniform, although Arctic-only SRM has also been considered[6,8]. Optimization with three degrees of freedom of spatial variation was introduced in ref. 11 for two different climate metrics, but trade-offs between these metrics were not quantitatively considered. Introducing multiple spatial and temporal degrees of freedom has the potential to improve how well SRM can compensate for CO_2-induced climate change, and thus reduce concerns over the resulting regional inequalities. Whereas temperature responds relatively slowly to changes in radiative forcing (because of oceanic thermal inertia), the land–sea temperature contrast responds rapidly[12,13], which in turn affects monsoonal precipitation. Introducing a seasonal dependence thus has the potential to partially decouple the temperature and precipitation responses to SRM; we minimize monthly-mean rather than annual-mean changes to ensure that any changes in the seasonal cycle caused by seasonal forcing are not masked by annual averaging.

We assume as in refs 3,9 that impacts related to climate change are a quadratic function of the deviations of temperature and precipitation relative to a pre-industrial baseline, with each normalized by the standard deviation of inter-annual variability. We use the sum of squares of these normalized deviations as our primary optimization metric, equally weighting temperature and precipitation, and consider both the global average and the worst-case value over any region. The true relationship between climate changes and climate impacts is not known, although a quadratic function is often used as a plausible proxy[14,15], in part for analytical tractability. A different choice of damage function would affect the quantitative results, but would probably not affect the qualitative conclusions that increasing the degrees of freedom available for climate engineering can reduce the severity of trade-offs between objectives.

By introducing spatio-temporal tailoring of the distribution of insolation reduction, the choice of different weightings between variables strongly influences the climate that results from the optimization. We consider three trade-offs: the trade-off between minimizing global root-mean-square (r.m.s.) climate changes and minimizing residual changes at the worst-off location, the trade-off between minimizing global r.m.s. climate changes and the average solar reduction required to do so, and the trade-off between minimizing global r.m.s. climate changes and maximizing Northern Hemisphere September sea ice, for a given average solar reduction. Several other cases are noted in the Supplementary Information.

[1]Control and Dynamical Systems, California Institute of Technology, 1200 E. California Blvd., Pasadena, California 91125, USA, [2]School of Engineering and Applied Sciences and Kennedy School of Government, Harvard University, Cambridge, Massachusetts 02138, USA, [3]Department of Global Ecology, Carnegie Institution, Stanford, California 94305, USA. *e-mail: macmardg@cds.caltech.edu.

We explore the potential of these optimizations using a fully-coupled atmosphere–ocean general circulation model (AOGCM), HadCM3L (ref. 16). To avoid being specific to a particular method of implementing SRM, we modify the incoming solar radiation directly, as a proxy for any method that reduces insolation. Any implementation of SRM would of course introduce other extra complications that would need to be considered; furthermore, the potential benefits of tailoring the forcing distribution would likely be smaller in the real world than in this model because of uncertainty in the climate response. We choose Legendre polynomials (constant, linear and quadratic) in the sine of latitude for the spatial distribution of forcing, as in ref. 11, and raised-cosines peaking in each season for the temporal distribution (Fig. 1; the temporal patterns are chosen so that they sum to a uniform distribution). Although these variations may be difficult to achieve in practice, it is premature to presume today what variations might ultimately be achievable. If SRM were implemented using stratospheric aerosols, for example, the choice of aerosol injection timing and latitude could introduce some (limited) temporal and spatial variability in aerosol concentrations and, hence, in the solar reduction[17,18]; engineered particles[18] or space-based systems might enable more control over the distribution of solar reduction. Marine cloud brightening approaches might allow some influence on the longitudinal distribution of forcing as well; indeed multiple approaches might simultaneously be used to balance different objectives.

The climate response is computed separately for each of the spatial and temporal patterns shown in Fig. 1 (see Methods). Estimating the response to any combination of these patterns as a linear superposition of the responses to individual patterns is a good approximation for this model, and is easily verified; see Supplementary Figs S1–S3, see also refs 3,11. Assuming linearity, optimization is straightforward (see Methods). We focus only on the long-term climate response to a doubling of CO_2; the results would differ during a transient (non-equilibrium) CO_2 increase owing to the different pattern of climate change resulting primarily from the ocean thermal inertia. A similar approach as considered here could be used to understand the best forcing distribution at any particular time during the transient.

Whereas refs 3,9 optimize over Giorgi regions[19], here we optimize at the grid-cell level, as spatial-averaging can mask an increase in part of a region which is offset by decreases elsewhere within the region. The appropriate spatial scale is not obvious, both for economic reasons (for example, the average rainfall within a watershed matters), and because of the limits of model resolution (grid-scale information is not reliable). However, the general conclusions are not dependent either on this choice, or on whether monthly-mean or annual-mean changes are considered (Supplementary Table S1).

Figure 2 illustrates the trade-off between minimizing the global r.m.s. normalized temperature and precipitation changes, and those at the worst-case location. Spatial and seasonal variation in solar reduction can be used to achieve a 30% reduction in the worst-case residual (a factor of two in quadratic impacts), without a significant degradation in compensating global r.m.s. climate changes. In contrast, with uniform solar reduction, a small reduction in the worst-case residual beyond the level where the global r.m.s. is minimized comes at the expense of a significant increase in the global r.m.s. climate changes.

Note that with no constraint imposed on the average insolation reduction, as in Fig. 2, then both non-uniform and uniform solar reduction yield similar reductions in the global r.m.s. normalized temperature and precipitation changes. Uniform solar reduction tends to overcompensate CO_2-induced temperature changes in the tropics relative to the poles[6,11], and a small improvement in r.m.s. temperature can be achieved by shifting the insolation reduction towards the poles (Supplementary Fig. S7). In this model, compensating increased CO_2 with uniform solar reduction leads to wetter precipitation residuals in the tropics and drier elsewhere. Overcooling the tropics while undercooling elsewhere would slightly reduce these precipitation residuals (Supplementary Fig. S8).

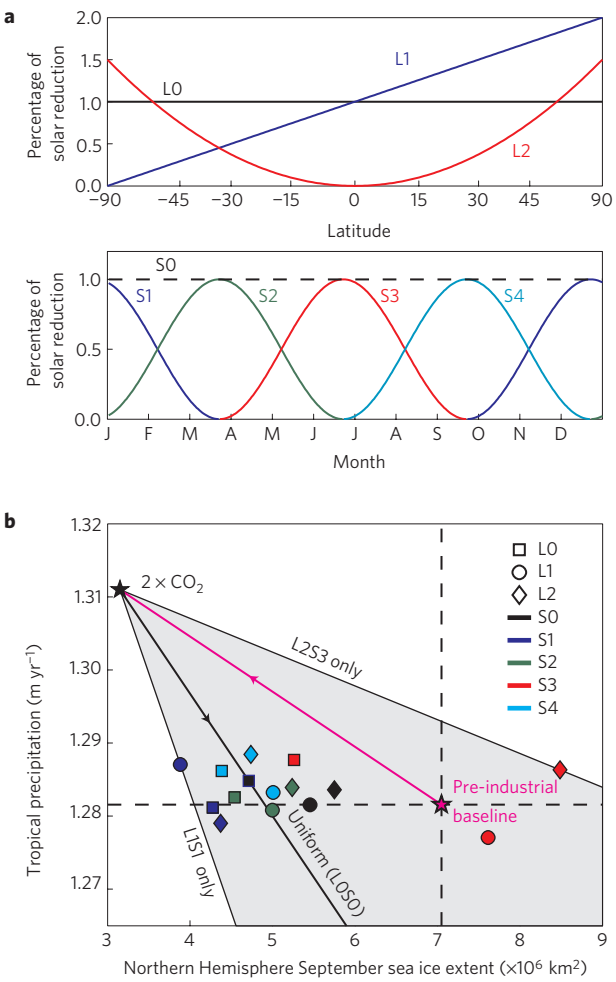

Figure 1 | Solar reduction forcing patterns and motivation. a, Spatial (L0, L1, and L2 for uniform, linear and quadratic) and seasonal variations (S0 for uniform and S1–S4 for each season). These are normalized to 1% average solar reduction in plotting responses in **b**, which illustrates the trade-off between two variables: Northern Hemisphere September sea ice extent, and annual-average tropical precipitation, averaged over 30° S–30° N. The magenta line connects the baseline and $2 \times CO_2$ cases to illustrate the 'direction' that CO_2 forcing alters the climate. The black line illustrates the effect of uniform solar reduction on these variables, while the shaded region indicates the set achievable with a linear combination of forcings.

Further trade-offs are illustrated in Fig. 3. The first is the reduction in climate changes possible for smaller values of the average solar insolation reduction (spatially- and seasonally-averaged). This would probably result in reduced side effects and risks of SRM, such as ozone depletion or effects on cirrus in the case of stratospheric aerosols[20]. For example, with an average insolation reduction of only 1.5%, the r.m.s. normalized temperature and precipitation residual is 30% smaller than when only uniform solar reduction is used (29% of the $2 \times CO_2$ case, versus 40% of the $2 \times CO_2$ case), giving a factor of two reduction in quadratic impacts. Similarly, a 50% reduction in r.m.s. normalized temperature and precipitation residuals (factor of four in quadratic impacts) can be obtained using 30% lower average solar reduction; see also Supplementary Fig. S6. These result from the ability to focus solar reductions where and when they are most important for minimizing

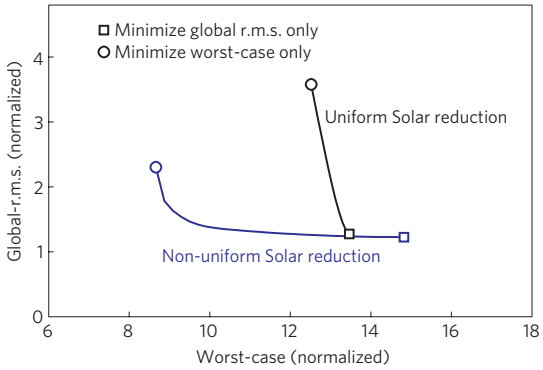

Figure 2 | The trade-off between minimizing the global-r.m.s. normalized temperature and precipitation changes, and minimizing the worst-case change over any grid-cell. Both are expressed in number of standard deviations of inter-annual variability; the end-points of each line indicate the minimum of each metric with no weighting on the other. With uniform solar reduction, the worst-case is minimized by increasing the insolation reduction beyond the level that minimizes the global-r.m.s. With non-uniform solar reduction, the minimum worst-case residual is 30% lower than with uniform solar reduction, and most of this improvement can be obtained without significantly increasing either the global-r.m.s. residual or the average solar reduction used.

the global r.m.s. climate changes, for example, in high-latitude summer regions. Temperature sensitivity to solar reduction in high latitudes is higher than for the global average, as discussed in ref. 6.

Whereas different climate metrics were introduced in ref. 3, uniform solar reduction provides limited ability to generate different climates. By varying the spatial and seasonal distribution, the choice of how to weight different climate impacts can lead to quite different outcomes. Figure 3a illustrates the trade-off in varying the relative emphasis on temperature versus precipitation in the presence of a constraint on average solar reduction. The choice of metrics is not limited to restoring the climate to some baseline; Fig. 3b illustrates the trade-off between minimizing the deviations in temperature and precipitation from a pre-industrial baseline, and maximizing the Northern Hemisphere September (annual minimum) sea ice extent. With an average solar reduction of only 0.5%, it is possible to recover pre-industrial sea ice extent (from $2 \times CO_2$) while still reducing temperature and precipitation changes by more than that which a 0.5% uniform solar reduction would achieve. These types of trade-off raise the question of what the balance should be for these various metrics.

The results obtained here with our model indicate that spatial and temporal variation in solar insolation reduction can be used to improve the compensation between the climate response due to SRM and that due to increased greenhouse forcing. We do not address how one might achieve the desired forcing distributions. Nonlinearities and non-equilibrium conditions will also affect the quantitative results; a real-world optimization would also be based on uncertain model estimates and hence may not lead to the same level of compensation of climate effects suggested in these simulations.

With no constraint on the average solar reduction, the improvements in minimizing r.m.s. temperature and precipitation changes are modest, but significant improvements are possible in minimizing the worst-case response, of particular interest for managing regional inequalities. Furthermore, the use of spatially and seasonally varying reductions in solar insolation permits much better climate compensation with a small reduction in average solar insolation, of relevance to reducing side-effects and risks of SRM, such as ozone depletion. The trade-offs between different objectives are not limited to restoring the climate to a current or pre-industrial baseline; it may be useful, for example, to overcompensate Northern

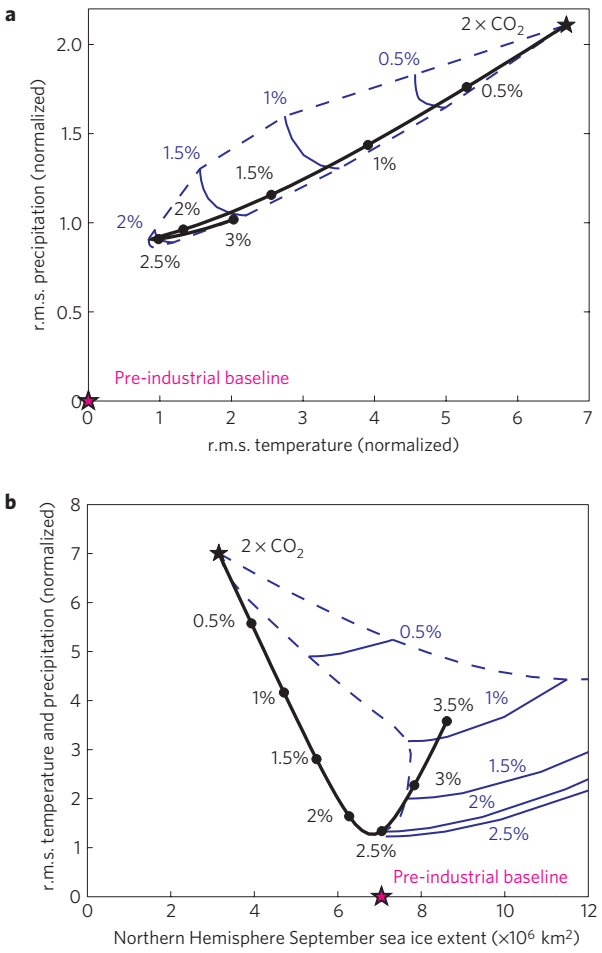

Figure 3 | Trade-offs between different objectives. a, Minimizing r.m.s. normalized temperature, precipitation, or some combination. **b**, Maximizing Northern Hemisphere September sea ice extent and minimizing combined r.m.s. normalized temperature and precipitation residuals. Both trade-offs are shown for increasing uniform solar reduction (solid black line, circles indicate solar reduction), and non-uniform solar reduction for different relative weightings. (**a**) Weighting only temperature (upper dashed line), only precipitation (lower dashed line), or some combination (connecting lines, shown at constant average solar reduction). (**b**) Weighting only sea ice (upper dashed line), only temperature and precipitation (lower dashed line), or some combination (connecting lines, shown at constant average solar reduction); similarly in **a**. The multiple degree of freedom case allows greater reductions if the average solar reduction is constrained, and results in climates that are not achievable with only uniform solar reduction.

Hemisphere sea ice to reverse long-term changes in the Arctic, while still reducing climate impacts globally. More degrees of freedom enlarges the trade space of possible climate outcomes and raises the question of what are the preferred trades? Many other variables could ultimately be considered in an optimization, with a regionally-specific relative emphasis. In summary, decisions involving SRM do not need to be reduced to a single 'global thermostat'.

Methods

We use GCM simulations to estimate the climate response due to a doubling of CO_2, and to estimate the climate response for each of the spatio-temporal patterns of insolation reduction shown in Fig. 1. Assuming linearity, the residual climate changes can then be estimated for any combination of these patterns, as a linear combination of the response (equation (1) below). Minimizing a quadratic function of climate changes relative to a pre-industrial baseline results in a weighted least-squares optimization. Including a constraint on the average insolation reduction yields a constrained least-squares problem that is also

straightforward to solve; it is also straightforward to minimize the worst-case climate residuals over any location.

We use the HadCM3L coupled AOGCM, which has resolution of 3.75° in longitude by 2.5° in latitude in both the atmosphere and ocean, with 19 vertical levels in the atmosphere and 20 in the ocean[16]. This is the same model, with a slightly different configuration, that has been used for simulating SRM in ref. 7, and for exploring regional effects and the optimization of SRM in refs 3,9. HadCM3 is a participant in the Geoengineering Model Intercomparison Project[21]; intercomparisons show HadCM3 achieves similar results to other AOGCMs in simulating geoengineering by reducing the solar constant (B. Kravitz, personal communication). Note that HadCM3 underestimates both present day September sea ice cover[22] and projected future relative reductions[23].

A case with no added SRM and pre-industrial CO_2 (278 ppm) is used both to define the 'baseline' or desired climate, and to estimate the natural climate variability for normalization. A case with $2\times CO_2$ is used to define the perturbed climate that SRM is intended to compensate. The climate response for each forcing distribution in Fig. 1 is simulated independently. (Note that the solstice timing is exact, but we use fixed 3-month separations on a 360-day calendar year, resulting in a small timing offset relative to the equinoxes due to the eccentricity of Earth's orbit.) For each applied radiative forcing pattern, and for the $2\times CO_2$ case, we compute the monthly means over the second 100 years of a 200-year simulation to minimize errors in estimating the long timescale behaviour. (This is sufficient such that the errors in estimating responses due to natural variability are small compared to the errors due to nonlinearity; for example, the error bars in Fig. 1b are negligible.) A similar approach could be used to estimate transient climate response with ensemble averaging to minimize errors.

The monthly-mean temperature and precipitation differences between the $2\times CO_2$ case and the baseline case for all m grid cells can be concatenated into a single vector $\mathbf{b}\in\mathbb{R}^{24m}$, where the temperatures and precipitations are normalized by the standard deviations of the respective interannual natural variabilities. For r.m.s. minimization, each grid cell is also weighted by area. Similarly, the influence vector of normalized climate responses for all n patterns of solar reduction can be concatenated into a matrix $A\in\mathbb{R}^{24m\times n}$, where each column describes the climate influence due to a particular spatio-temporal pattern of solar insolation reduction, and each row is the normalized monthly temperature or precipitation change for a given grid cell. Assuming linearity, the residual response after SRM, $\mathbf{z}\in\mathbb{R}^{24m}$, will be of the form

$$\mathbf{z}=\mathbf{b}-A\mathbf{u} \tag{1}$$

where the forcing amplitude corresponding to each solar reduction pattern is contained in the vector $\mathbf{u}\in\mathbb{R}^{n}$.

The constraint that the solar insolation never be increased can be written as $C\mathbf{u}\le 0$, with each row of the matrix C corresponding to the constraint that solar insolation be reduced at a particular latitude and time of year. (Thus c_{ij} is the amplitude of the jth basis vector of forcing at the ith latitude and time; in practice, it is sufficient to enforce this at only a few times of the year and at a few latitudes.) A constraint on the total average solar reduction can also be included in C. The resulting constrained least-squares problem can be efficiently solved with quadratic programming:

$$J^{*}=\min_{\mathbf{u}}\left\{\mathbf{u}^{\mathrm{T}}(A^{\mathrm{T}}A)\mathbf{u}+2\mathbf{b}^{\mathrm{T}}A\mathbf{u}\right\}\quad\text{such that}\quad C\mathbf{u}\le 0 \tag{2}$$

Provided that a constraint is included on the total solar insolation reduction, it is also straightforward to include in the same framework variables one might wish to maximize rather than minimize, such as sea ice extent.

We also consider the solar reduction pattern that minimizes the worst-case deviation of normalized climate response in any grid-cell:

$$J^{*}=\min_{\mathbf{u}}\max_{i}|(\mathbf{b}-A\mathbf{u})_{i}|\quad\text{such that}\quad C\mathbf{u}\le 0 \tag{3}$$

where $(\cdot)_i$ refers to the ith element of the vector. Figure 2 is obtained by optimizing as in (2) with additional constraints $A\mathbf{u}\le\alpha-\mathbf{b}$ and $-A\mathbf{u}\le\alpha+\mathbf{b}$, where α is the allowable worst-case change.

Received 9 May 2012; accepted 18 September 2012; published online 21 October 2012

References

1. Keith, D. Geoengineering the climate: History and prospect. *Annu. Rev. Energ. Environ.* **25,** 245–284 (2000).
2. Crutzen, P. J. Albedo enhancement by stratospheric sulfur injections: A contribution to resolve a policy dilemma? *Climatic Change* **77,** 211–219 (2006).
3. Moreno-Cruz, J., Ricke, K. & Keith, D. W. A simple model to account for regional inequalities in the effectiveness of solar radiation management. *Climatic Change* **110,** 649–668 (2011).
4. Govindasamy, B. & Caldeira, K. Geoengineering Earth's radiation balance to mitigate CO_2-induced climate change. *Geophys. Res. Lett.* **27,** 2141–2144 (2000).
5. Rasch, P. J., Crutzen, P. J. & Coleman, D. B. Exploring the geoengineering of climate using stratospheric sulfate aerosols: The role of particle size. *Geophys. Res. Lett.* **35,** L02809 (2008).
6. Caldeira, K. & Wood, L. Global and Arctic climate engineering: Numerical model studies. *Phil. Trans. R. Soc. A* **366,** 4039–4056 (2008).
7. Lunt, D. J., Ridgwell, A., Valdes, P. J. & Seale, A. Sunshade World: A fully coupled GCM evaluation of the climatic impacts of geoengineering. *Geophys. Res. Lett.* **35,** L12710 (2008).
8. Robock, A., Oman, L. & Stenchikov, G. Regional climate responses to geoengineering with tropical and Arctic SO_2 injections. *J. Geophys. Res.* **113,** D16101 (2008).
9. Ricke, K. L., Granger Morgan, M. & Allen, M. R. Regional climate response to solar-radiation management. *Nature Geosci.* **3,** 537–541 (2010).
10. Bala, G., Duffy, P. B. & Taylor, K. E. Impact of geoengineering schemes on the global hydrological cycle. *Proc. Natl Acad. Sci. USA* **105,** 7664–7669 (2008).
11. Ban-Weiss, G. A. & Caldeira, K. Geoengineering as an optimization problem. *Environ. Res. Lett.* **5,** 034009 (2010).
12. Dong, B., Gregory, J. M. & Sutton, R. T. Understanding land-sea warming contrast in response to increased greenhouse gases. Part I: Transient adjustment. *J. Clim.* **22,** 3079–3097 (2009).
13. MacMynowski, D. G., Shin, H-J. & Caldeira, K. The frequency response of temperature and precipitation in a climate model. *Geophys. Res. Lett.* **38,** L16711 (2011).
14. Nordhaus, W. *A Question of Balance: Weighing the Options on Global Warming Policies* (Yale Univ. Press, 2008).
15. Weitzman, M. What is the damages function for global warming—and what difference might it make? *Clim. Change Econom.* **1,** 57–69 (2010).
16. Jones, C. A fast ocean GCM without flux adjustments. *J. Atm. Oceanic Tech.* **20,** 1857–1868 (2003).
17. English, J. M., Toon, O. B. & Mills, M. J. Microphysical simulations of sulfur burdens from stratospheric sulfur geoengineering. *Atmos. Chem. Phys.* **12,** 4775–4793 (2012).
18. Keith, D. W. Photophoretic levitation of engineered aerosols for geoengineering. *Proc. Natl Acad. Sci. USA* **107,** 16428–16431 (2010).
19. Giorgi, F. & Francisco, R. Uncertainties in regional climate change prediction: A regional analysis of ensemble simulations with the HADCM2 coupled AOGCM. *Clim. Dynam.* **16,** 169–182 (2000).
20. The Royal Society *Geoengineering the Climate: Science, Governance and Uncertainty* (Royal Society, 2009).
21. Kravitz, B. *et al.* The Geoengineering Model Intercomparison Project (GeoMIP). *Atmos. Sci. Lett.* **12,** 162–167 (2011).
22. Holland, M. M., Serreze, M. C. & Stroeve, J. The sea ice mass budget of the Arctic and its future change as simulated by coupled climate models. *Clim. Dynam.* **34,** 185–200 (2010).
23. Boe, J. L., Hall, A. & Qu, X. September sea-ice cover in the Arctic Ocean projected to vanish by 2100. *Nature Geosci.* **2,** 341–343 (2009).

Author contributions

D.G.M. and D.W.K. conceived the project, D.G.M. carried out the analysis with contributions from B.K. All authors wrote the paper.

Additional information

Supplementary information is available in the online version of the paper. Reprints and permissions information is available online at www.nature.com/reprints. Correspondence and requests for materials should be addressed to D.G.M.

Competing financial interests

The authors declare no competing financial interests.